Unmanned Systems, Vol. 0, No. 0 (2023) 1–13

Unmanned Systems, Available online 12 March 2025
DOI:10.1142/s2301385026500081

Enhancing Quadrotor Resilience in Outdoor Operations with Real-time Wind Gust Measurement by using LiDAR

Zohaib Latif[a], James Ferris Whidborne[a], Aamer Iqbal Bhatti[b],Amir Shahzad[c], Raza Samar[c]

[a] *Cranfield University, Milton Keynes MK43 0AL, United Kingdom*
E-mail: engr.zlatif@gmail.com

[b] *King Fahd University of Petroleum & Minerals, Dhahran, Saudi Arabia*

[c] *Centres of Excellence in Science and Applied Technologies, Islamabad*

Unmanned Aerial Vehicles (UAVs) encounter wind gusts during outdoor operations, impacting their position holding, particularly for quadrotors. This vulnerability is amplified during the autonomous docking to outdoor charging stations. The integration of real-time wind preview information for UAV gust rejection control has become more feasible with advances in remote wind sensor technologies like LiDAR. In this study, a ground-based LiDAR system is proposed to predict wind gusts at the landing site of quadrotors. The acquired wind preview data is subsequently utilised by the Model Predictive Control (MPC) to effectively mitigate disturbances. To validate the proposed methodology, a non-linear simulation environment has been established using LiDAR data collected from comprehensive field tests. The results demonstrate a notable improvement in the system performance compared to benchmark results. This research underscores the practical utility of real-time wind preview information, facilitated by LiDAR technology, in enhancing the overall operational resilience of UAVs, especially quadrotors, during challenging environmental conditions.

Keywords: Quadrotor, Outdoor Operations, Wind Gust Measurement, LiDAR, MPC

1. Introduction

Unmanned Air Vehicles (UAVs) have gained significant popularity over the past few decades due to their versatile applications, ranging from military operations to public safety. Nowadays, UAVs are also used for commercial purposes such as image and data acquisition in disaster areas, traffic surveillance, communication delays, map building, search and rescue, and more. However, quadrotors face a challenging task of maintaining baseline performance during outdoor autonomous operations. Their small mass makes them vulnerable to wind gusts, which can significantly alter their intended flight trajectory, posing a safety risk, especially during the most vulnerable tasks like landing and take-off from a charging station. Therefore, a gust resilient control system is necessary to ensure the reliable and safe autonomous operations of UAVs. The flight control system should be capable of sensing real-time wind and adjusting the position and attitude of the UAV to compensate for the disturbance effects.

In most quadrotor gust rejection systems, the wind is considered an external disturbance, and a model-based robust observer or filter is used to estimate the wind disturbance [1]. A suitable feedback control law then compensates for its effects. For instance, [2] developed a generalized extended state estimator to predict wind disturbance and utilized an attitude tracking back-stepping control method to counteract its effects. The estimation of wind disturbance is done using Kalman filtering methods [3–5], disturbance observer approach [3,6–8], and active disturbance rejection control [9, 10] along with the control law.

However, in all these methods, gust is estimated from the measurement of the resulting quadrotor movement, which adds a lag in the estimation and compensation process, ultimately reducing the potential performance improvement. Additionally, the estimated wind can be contaminated by the wind produced by the quadrotor propellers. Moreover, onboard wind estimation increases the computation load, which is another limitation for small UAVs. In the aerospace industry, LiDAR (Light Detection and Ranging) has been used to estimate wind disturbances [11].

LiDAR technology can be used to estimate wind speed by measuring the Doppler shift in the frequency of light that is backscattered. Several studies have utilized LiDAR for improving the gust rejection performance of UAVs. For example, in [12], an onboard LiDAR mounted on the nose of an aircraft was used to investigate the characteristics of wake vortices and enhance the gust rejection performance. In [13], the LiDAR system mounted on a multi-rotor UAV provided separate line of sight measurement to construct the wind vector. An H_∞ based controller that utilizes on-

board LiDAR information was used in [14] for autonomous landing of aircraft. LiDAR-based wind data for a year-long measurement is used in [15] to evaluate the tendency of gusts that induce wind power ramps.

In this work, a ground-based LiDAR unit is utilized to generate wind preview at the landing site for autonomous operation of quadrotors. The wind information obtained is used to compute the necessary control action to compensate for its effects and improve the gust rejection capability. The Model Predictive Control (MPC) formulation is used as a suitable methodology that incorporates the LiDAR information. One of the advantages of using a ground-based LiDAR unit is that it has no physical connection to the autonomous UAV and hence does not limit its flight-envelope. Additionally, integrating the wind preview system with the ground charging system could ideally avoid the weight penalty. A similar approach has been employed by [16], focusing primarily on performance metrics and robustness.

The Model Predictive Control (MPC) technique is an optimal control method that utilizes the current state information and predicts the system evolution over a desired future horizon. It then solves an online optimization problem to generate optimal control sequences that result in constraint satisfactions. Initially, MPC was widely used in the process industry where the change in the plant dynamics is slow. However, recent developments in computing capacity and hardware have significantly reduced the difficulties in implementing modern control techniques for fast systems. As a result, MPC is gaining popularity in the aero industry due to its ability to handle the constraints of multivariable systems. Additionally, its ability to handle and mitigate the impact of measured disturbance makes it more suitable for aero applications. The wind disturbance previewed by the on-ground LiDAR is utilized in the MPC formulation to optimally reject its effects. By incorporating real-time wind preview information into the MPC framework, the proposed methodology can effectively mitigate disturbances and enhance the operational resilience of quadrotors in difficult environmental conditions.

The main contributions of this work are summarized as follows:

(1) Development of a linear MPC explicitly designed to account for wind effects on a quadrotor UAV.
(2) Novel integration of wind data estimated from a ground-based LiDAR system directly into the MPC framework as a measured disturbance, avoiding the limitations of traditional feedforward compensation methods.
(3) Demonstrate significant performance improvement over benchmark results, validating the effectiveness of the proposed approach in enhancing UAV stability in outdoor environments.

The paper is structured as the following manner. Section 2 provides a brief discussion of the non-linear and linear models of the UAV and wind preview model, which is essential for understanding the subsequent sections. Section 4 offers a detailed explanation of the design steps for the MPC, which is a crucial aspect of this paper. In Section 4, the hovering control of the UAV is realized using the MPC, which is a significant contribution of this paper. Section 5 presents a comprehensive discussion of the results obtained from the simulations, providing readers with a clear understanding of the effectiveness of the proposed approach. Finally, in Section 6, the authors draw insightful conclusions, which summarize the key findings of this paper.

2. Mathematical Model

A quadrotor is a UAV that utilizes four rotors for its propulsion. Mathematical modeling of the quadrotor encompasses capturing its motion, as well as the forces and moments that act upon it. Extensive literature exists on the non-linear model for the quadrotor. In this context, we provide a brief overview of both the non-linear and linear models for the quadrotor, which are crucial for the design of control systems.

2.1. *Non-Linear Model*

The non-linear model for the quadrotor is founded on the principles of classical control and mechanics theory. It utilizes a set of non-linear differential equations to express the quadrotor dynamics. These equations primarily focus on the quadrotor translational motion along the x, y, and z-axes, as well as its rotational motion around these axes (i.e., roll, pitch, and yaw). A quadrotor is effected by four independently varying speed rotors and has four control inputs (3 moments and 1 force), as shown in Figure 1, where $L = l(T_4 - T_2)$, $M = l(T_1 - T_3)$, $N = -\tau_1 + \tau_2 - \tau_3 + \tau_4$ and $T = T_1 + T_2 + T_3 + T_4$. Here, T_i is the thrust of ith rotor, l is the arm length and τ_i is the torque from ith rotor.

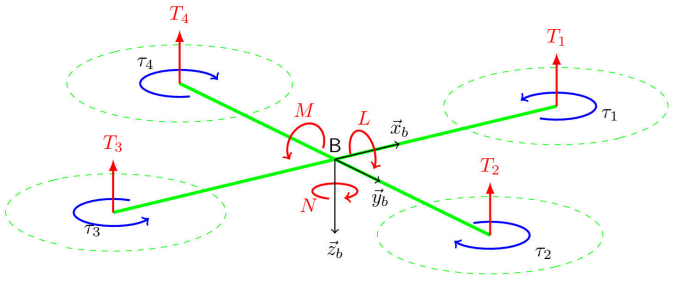

Fig. 1. Thrust, Forces and Moments on Quadrotor

The model makes several assumptions, including that the structure is rigid and symmetric, the inertia matrix is diagonal, ground effect is not considered, and body aerodynamic forces are neglected. The controller generates thrusts and moments about the body axes using rotors, which are

assumed to have rigid propeller blades and ignore rotor Coriolis forces, wind and drag effects, and motor dynamics.

The quadrotor attitude is expressed using the classical aerospace Euler angles (ϕ, θ, and ψ) which are strictly the Tait-Bryan angles (e.g. [17]). Hence the equations that describe the quadrotor translational motion along the x, y, and z-axes are as follows:

$$\begin{aligned} m\ddot{x} &= (\sin\psi\ \sin\phi + \cos\psi\ \sin\theta\ \cos\phi)T \\ m\ddot{y} &= (-\cos\psi\ \sin\phi + \sin\psi\ \sin\theta\ \cos\phi)T \\ m\ddot{z} &= -\cos\theta\ \cos\phi\ T + g \end{aligned} \tag{1}$$

where, m is the mass of the quadrotor and g is the gravitational acceleration. The rotational equation of motion in body axes are as follows:

$$\begin{aligned} I_x\dot{p} &= L - (I_z - I_y)qr \\ I_y\dot{q} &= M - (I_x - I_z)rp \\ I_z\dot{r} &= N - (I_y - I_x)pq \end{aligned} \tag{2}$$

where, I_x, I_y, and I_z are the moments of inertia. The relationships between the Euler angles are described by:

$$\begin{aligned} \dot{\phi} &= p + q\ \sin\phi\ \tan\theta + r\ \cos\phi\tan\theta \\ \dot{\theta} &= q\ \cos\phi - r\ \sin\phi \\ \dot{\psi} &= \frac{q\ \sin\phi + r\ \cos\phi}{\cos\theta} \end{aligned} \tag{3}$$

The state variables of the system are $\bar{\mathbf{x}} = [x\ y\ z\ u\ v\ w\ \phi\ \theta\ \psi\ p\ q\ r]$ and the control input $\bar{\mathbf{u}} = [T\ L\ M\ N]$ is the applied force and moment vector. For the simulations in this research, the Draganflyer X-Pro quadrotor shown in Figure 2 is used, with physical parameters as listed in Table 1.

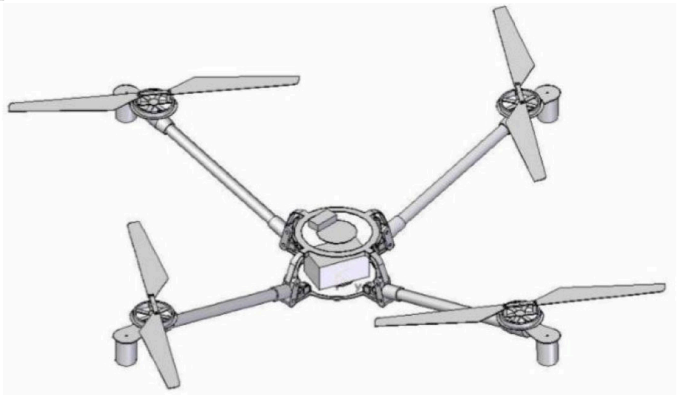

Fig. 2. Draganflyer X-Pro Quadrotor Ref. [18]

2.2. *Linear Model*

The non-linear model for the quadrotor is linearized using a numerical method in MATLAB by trimming it at a hovering position with no wind. The resulting state space representation of the linear model is as follows:

$$\begin{aligned} \delta\dot{\bar{\mathbf{x}}} &= \bar{A}\delta\bar{\mathbf{x}} + B\delta\bar{\mathbf{u}} + \bar{B}_w\bar{w} \\ \bar{y} &= \bar{C}\delta\bar{\mathbf{x}} \end{aligned} \tag{4}$$

In the given system, $\delta\bar{\mathbf{x}}$ is the perturbation in the state vector, while the system matrix is represented by $\bar{A}$. The input matrix due to the perturbed control input $\delta\bar{\mathbf{u}}$ is represented by $\bar{B}$, and $\bar{B}_w$ is the wind effector matrix. The measured wind is represented by $\bar{w}$, and the output is represented by $\bar{y}$, with $\bar{C}$ being the output matrix. The state space matrices are provided in Appendix 1.

Table 1. Physical Parameters of Draganflyer X-Pro

Parameter	**Value**
Mass	2.36 kg
Moment of inertia about x-axis	0.168 kg.m^2
Moment of inertia about y-axis	0.169 kg.m^2
Moment of inertia about z-axis	0.297 kg.m^2
Drag coefficient	1.05
Propeller arm length	0.45 m
Number of blades per propeller	2
Blade chord	0.04 m
Blade lift curve slope	5.5
Blade pitch	0.3025 rad
Blade zero lift drag coefficient	0.05
Blade drag coefficient due to angle of attack	0.7

2.3. *Wind Preview LiDAR*

A wind LiDAR is used to measure the wing disturbance. This LiDAR operates on the principle of Doppler effect and measures the shift in frequency of back-scattered light by air particles. Wind LiDARs are usually quite large and heavy, typically with a mass above 50 kg. The unit used in this study is a miniature continuous wave coherent LiDAR that based on infra-red range for measurements. This particular unit is a class 3b laser that measures $35 \times 25 \times 12$ cm and weighs approximately 5 kg. The LiDAR measures the line of sight wind velocity, and in order to reconstruct the wind vector, an alongside scanning process is required.

The unit would be located on the landing station for automated landing operation. The laser beam scans horizontally to construct the horizontal wind vector and, once upstream wind has been reconstructed, a wind propagation model is used to estimate the downstream wind in the earth axes. The study in [19] offers detailed information on the wind preview system components, measuring method, and experimental results. In this work, the wind data presented in Figure 3 from the field measurement is used to demonstrate the effectiveness of MPC for gust rejection.

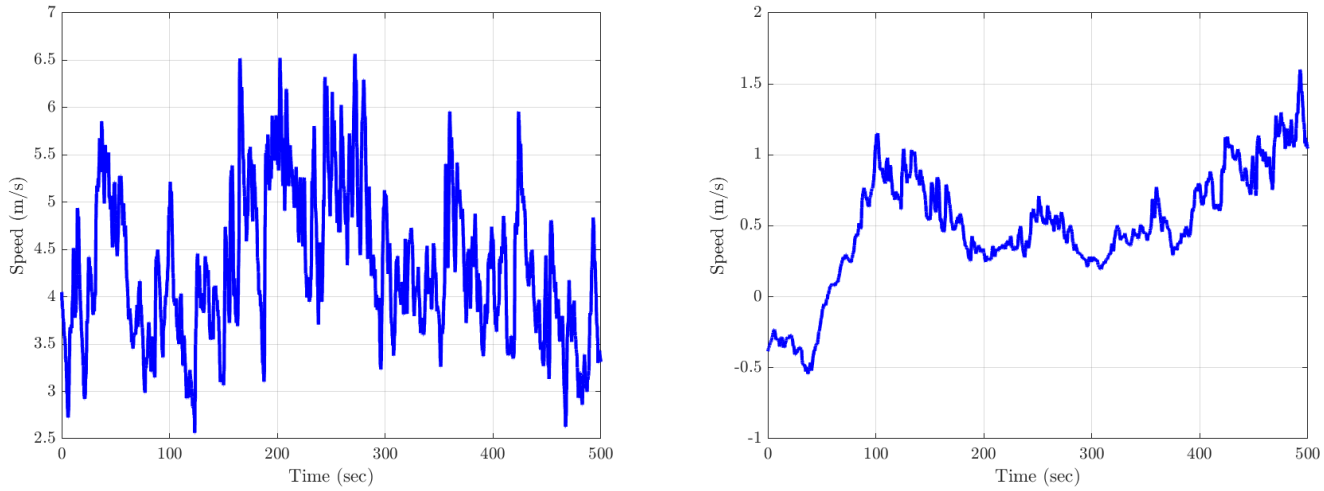

Fig. 3. Wind Speed along x and y-axis

3. Control Architecture

Figure 4 illustrates the control architecture of the nonlinear simulation environment. The MPC generates the control signal, which is then sent to the inner-loop PID controller to track the respective input. To determine the gains of the PID controllers, the Simulink in-built PID tuner is used, and the values are listed in Table 2. The output of the PID controllers are T, L, M and N, which correspond to thrust, pitch differential, roll differential, and yaw differential, respectively. The control allocation block is then used to combine and translate the control input into the rotational speed requirements for each propeller. To estimate the rotational rate of the quadrotor, which is not possible to access from the onboard sensors, a Kalman Filter (KF) is used. The KF also minimizes the process noise and measurement errors.

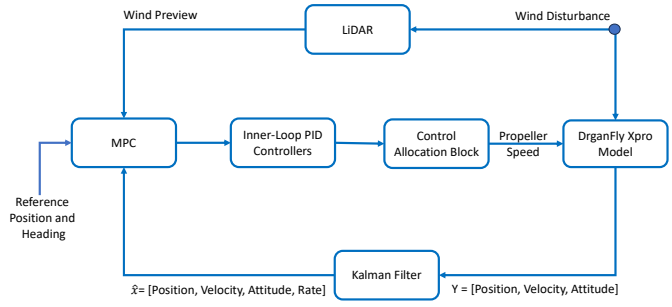

Fig. 4. Block Diagram of Control Architecture

Table 2. Inner-Loop PID Controller Gains

Control Channel	Proportional Gain	Integral Gain	Derivative Gain
Roll	5.89 Nmrad^{-1}s	0.13 Nmrad^{-1}	1.62 Nmrad^{-1}s
Pitch	5.89 Nmrad^{-1}s	0.13 Nmrad^{-1}	1.62 Nmrad^{-1}s
Yaw	2.44 Nmrad^{-1}s	0.08 Nmrad^{-1}	6.56 Nmrad^{-1}s
Altitude	5.89 Nm^{-1}	0.80 Nm^{-1}	8.72 Nm^{-1}s

4. MPC Formulation

The MPC is a feedback control approach that solves an optimization problem in real-time. The optimization algorithm computes the control input sequence over a finite-time horizon at each time step. The objective function is minimized, while ensuring that input, output, and/or state constraints are met. The first control input from the sequence is applied to the system, and the process is repeated recursively in a receding horizon manner at every sampling step. For the quadrotor, given an initial state x_0 at any time index k, the goal is to compute a finite horizon control input sequence $[u_0,\ u_1,\ u_2, ...u_{N-1}]$ that minimizes the finite horizon cost function.

$$J(u) = \sum_{k=0}^{N-1} \|y_k - y_k^{\text{ref}}\|_{Q_k}^2 + \|u_k\|_{R_k}^2 \tag{5}$$

subject to discrete time state space model:

$$\begin{aligned} x_{k+1} &= Ax_k + B_u u_k + B_w w_k \\ y_k &= Cx_k \end{aligned} \tag{6}$$

where $x_k \in \mathbb{R}^n$ is the state vector, $u_k \in \mathbb{R}^m$ is the input vector, $y \in \mathbb{R}^p$ is a vector of outputs which are to be

controlled, y^{ref} is the reference trajectory, N is the prediction horizon length. The weighting matrices Q_k and R_k are symmetric and semi-positive definite matrices. The primary control objective is to optimally regulate the system output to the reference trajectory. The objective function can be rewritten as:

$$J(u) = \|\mathbf{y} - \mathbf{y}^{\text{ref}}\|_Q^2 + \|\mathbf{u}\|_R^2 \tag{7}$$

where

$$\mathbf{y} = \begin{bmatrix} y_1 \\ y_2 \\ \vdots \\ y_N \end{bmatrix}, \quad \mathbf{y}^{\text{ref}} = \begin{bmatrix} y_1^{\text{ref}} \\ y_2^{\text{ref}} \\ \vdots \\ y_N^{\text{ref}} \end{bmatrix}, \quad \mathbf{u} = \begin{bmatrix} u_1 \\ u_2 \\ \vdots \\ u_N \end{bmatrix}$$

$$\mathbf{Q} = \begin{bmatrix} Q & 0 & \cdots & 0 \\ 0 & Q & \cdots & 0 \\ \vdots & \vdots & \ddots & \vdots \\ 0 & 0 & \cdots & Q \end{bmatrix}, \mathbf{R} = \begin{bmatrix} R & 0 & \cdots & 0 \\ 0 & R & \cdots & 0 \\ \vdots & \vdots & \ddots & \vdots \\ 0 & 0 & \cdots & R \end{bmatrix}$$

Equation 6 for prediction horizon N can also be written as:

$$\begin{aligned} x_1 &= Ax_0 + B_u u_0 + B_w w_0 \\ x_2 &= A^2 x_0 + ABu_0 + Bu_1 + AB_w w_0 + AB_w w_1 \\ &\vdots \\ x_N &= A^N x_0 + A^{N-1} B_u u_0 + A^{N-2} B_u u_1 + \cdots + B_u u_0 \\ &\quad + A^{N-1} B_w w_0 + A^{N-2} B_w w_1 + \cdots + B_w w_0 \end{aligned} \tag{8}$$

$$\begin{bmatrix} x_1 \\ x_2 \\ \vdots \\ x_N \end{bmatrix} = \underbrace{\begin{bmatrix} A \\ A^2 \\ \vdots \\ A^N \end{bmatrix}}_{\bar{T}} x_0 + \underbrace{\begin{bmatrix} B_u & 0 & \cdots & 0 \\ AB_u & B_u & \cdots & 0 \\ \vdots & \vdots & \ddots & \vdots \\ A^{N-1}B_u & A^{N-2}B_u & \cdots & B_u \end{bmatrix}}_{\bar{S}_u} \begin{bmatrix} u_0 \\ u_1 \\ \vdots \\ u_{N-1} \end{bmatrix}$$
$$+ \underbrace{\begin{bmatrix} B_w & 0 & \cdots & 0 \\ AB_w & B_w & \cdots & 0 \\ \vdots & \vdots & \ddots & \vdots \\ A^{N-1}B_w & A^{N-2}B_w & \cdots & B_w \end{bmatrix}}_{\bar{S}_w} \begin{bmatrix} w_0 \\ w_1 \\ \vdots \\ w_{N-1} \end{bmatrix}$$

$$\mathbf{x} = \bar{T}x_0 + \bar{S}_u \mathbf{u} + \bar{S}_w \mathbf{w} \tag{9}$$

The output vector

$$\mathbf{y} = \mathbf{C}\mathbf{x} \tag{10}$$

where

$$\mathbf{C} = \begin{bmatrix} C & 0 & \cdots & 0 \\ 0 & C & \cdots & 0 \\ \vdots & \vdots & \ddots & \vdots \\ 0 & 0 & \cdots & C \end{bmatrix}$$

The model evolution over the prediction horizon is based on the initial state without the intervention of control input. Consequently, the tracking error is defined as:

$$\mathbf{e} = \mathbf{y}^{\text{ref}} - \mathbf{C}\bar{T}x_0 \tag{11}$$

The cost function can be written as:

$$\begin{aligned} \mathbf{J} &= \left(\mathbf{C}\bar{S}_u\mathbf{u} + \mathbf{C}\bar{S}_w\mathbf{w} - \mathbf{e}\right)^T Q \left(\mathbf{C}\bar{S}_u\mathbf{u} + \mathbf{C}\bar{S}_w\mathbf{w} - \mathbf{e}\right) + \mathbf{u}^T R\mathbf{u} \\ &= \mathbf{u}^T H\mathbf{u} + \mathbf{u}^T F + \text{const.} \end{aligned} \tag{12}$$

where

$$H = \bar{S}_u^T \mathbf{C}^T Q \mathbf{C} \bar{S}_u + R, \quad F = 2(\bar{S}_u^T \mathbf{C}^T Q \mathbf{e} - \bar{S}_u^T \mathbf{C}^T Q \mathbf{C} \bar{S}_w \mathbf{w})$$

The constraints on the control inputs are $u_{\min} \leq u \leq u_{\max}$. For MPC, the constraints can be presented as:

$$\begin{bmatrix} -u \\ u \end{bmatrix} \leq \begin{bmatrix} -u_{\min} \\ u_{\max} \end{bmatrix}$$

For m numbers of inputs and prediction horizon N, the input constraints are defined as:

$$\begin{bmatrix} -I_{mN} \\ I_{mN} \end{bmatrix} \mathbf{u} \leq \begin{bmatrix} -\mathbf{u}_{\min} \\ \mathbf{u}_{\max} \end{bmatrix}$$
$$G\mathbf{u} \leq W$$

The above formulation has resulted in the transformation of the MPC problem into a QP problem with an unknown $\mathbf{u}$. In other words, the QP problem that needs to be solved is:

$$\min \left[\frac{1}{2}\mathbf{u}^T H\mathbf{u} + f^T\mathbf{u}\right], \quad \text{where} \quad f = -\frac{1}{2}G \tag{13}$$

$$\text{subject to:} \tag{14}$$

$$G\mathbf{u} \leq W \tag{15}$$

The above QP problem can be solved online at each sampling step by the interior point method or using MATLAB function, quadprog.

4.1. *Weight Selection*

It is important to establish a foundation for control design before delving into weight selection for MPC. The primary goal of MPC is to optimize system performance by manipulating control inputs over a finite prediction horizon. Therefore, it is essential to have a good understanding of quadrotor dynamics, external disturbances, and a well-defined cost function that can handle these issues. This subsection focuses on the formulation of a cost function, which is critical for a strategic weight selection process. The

emphasis is on balancing control objectives, such as minimizing effort, ensuring tracking accuracy, and enhancing stability in the face of wind disturbances during quadrotor position holding. Based on these objectives, the weighting parameters (Q and R matrices) were selected iteratively through trial-and-error to achieve the desired balance between control performance and actuator effort. This iterative approach ensured the controller effectively mitigated wind disturbances during the critical hovering phase over the landing deck. The final selected weights for MPC are as follows:

$$Q = \text{diag}(2,\ 1.5,\ 0.1,\ 1,\ 1,\ 1,\ 1,\ 1,\ 1,\ 1) \tag{16}$$

$$R = \text{diag}(2,\ 1,\ 1,\ 1) \tag{17}$$

The cost function mentioned above is used to solve the MPC problem, and the detailed results are presented and discussed in the next section.

5. Results and Discussion

To validate the designed algorithm, the proposed control law is implemented in a non-linear simulation environment. The simulation is conducted for two different scenarios. In the first case, the baseline performance of the control design is tested without wind effects, while the second case illustrates the effectiveness of the control algorithm with measured wind. The external disturbances used in the simulation are the measured wind values presented in Section 2.3, and the results are compared to a PID-based feedforward control law presented in [19].

5.1. *Case 1*

For the first case, the linear model of the UAV given in (2.2) is utilized to ensure the baseline performance of the system under ideal conditions. The attitude (roll, pitch, and yaw) and height command for the inner control system, as designed by MPC, are shown in Figure 5. Figure 6 shows that the UAV is tracking is reference value within 3 s with minimal overshoot.

5.2. *Case 2*

In the second case, the control algorithm is assessed under wind disturbances to evaluate its effectiveness. The wind velocities along the x and y-axis are previewed, as shown in Figure 3. The objective is to maintain the position of the UAV at a height of 10 meters above the landing deck, despite the wind disturbances. The effectiveness of the control design is assessed by comparing the results with and without wind preview data.

To compensate for the lateral and longitudinal wind disturbances, the quadrotor changes the pitch and roll demand. Figure 7 shows the input demand for the inner loop controllers, which are generated by MPC. The figure shows how the pitch and roll demand change to compensate for the wind disturbances. The outputs in Figure 8 demonstrate that the position holding performance of the quadrotor with wind preview data is significantly improved, with very minimal error. It can be seen that the quadrotor is able to maintain its position and altitude despite the wind disturbances.

Moreover, the designed control law is compared with the benchmark results presented in [19], as shown in Figure 9. The lateral and longitudinal wind profiles obtained from LiDAR are considered, assuming no vertical wind. The deviation from the quadrotor's hovering position along the x and y axes is compared with the benchmark study. The results show that the deviation is minimal, demonstrating the effectiveness of the proposed control algorithm in mitigating wind disturbances and maintaining the quadrotor's position and altitude.

6. Conclusion

In conclusion, this paper presents a novel control algorithm based on MPC for quadrotor position holding. The effectiveness of the proposed control algorithm is demonstrated through simulation studies conducted under different scenarios. The simulation results show that the MPC algorithm is effective in maintaining the position and altitude of the quadrotor under ideal and wind-disturbed conditions. The designed control law is compared with a benchmark control algorithm, and it is shown that the proposed control algorithm outperforms the benchmark algorithm in terms of position and altitude tracking accuracy. The proposed control algorithm is designed to handle external disturbances such as wind and is formulated to balance control objectives, such as minimizing effort, ensuring tracking accuracy, and enhancing stability. The cost function used in the MPC algorithm is designed to be robust and capable of handling quadrotor dynamics and external disturbances. The MPC algorithm generates attitude and height commands for the inner control system that are used to compensate for lateral and longitudinal wind disturbances. These commands are shown to be effective in maintaining the position and altitude of the quadrotor. Overall, the results of this study demonstrate the effectiveness of the proposed control algorithm for quadrotor position holding. The proposed control algorithm can be used in various applications where quadrotors are required to maintain their position and altitude accurately and robustly.

7. Future Work

Future work will focus on testing the proposed control methodology in a wider range of simulation environments to validate its generalizability and robustness. This will include evaluating various environmental scenarios, flight states, and an extended flight envelope to demonstrate its applicability. Additionally, experimental validation will be conducted to assess the methodology performance in

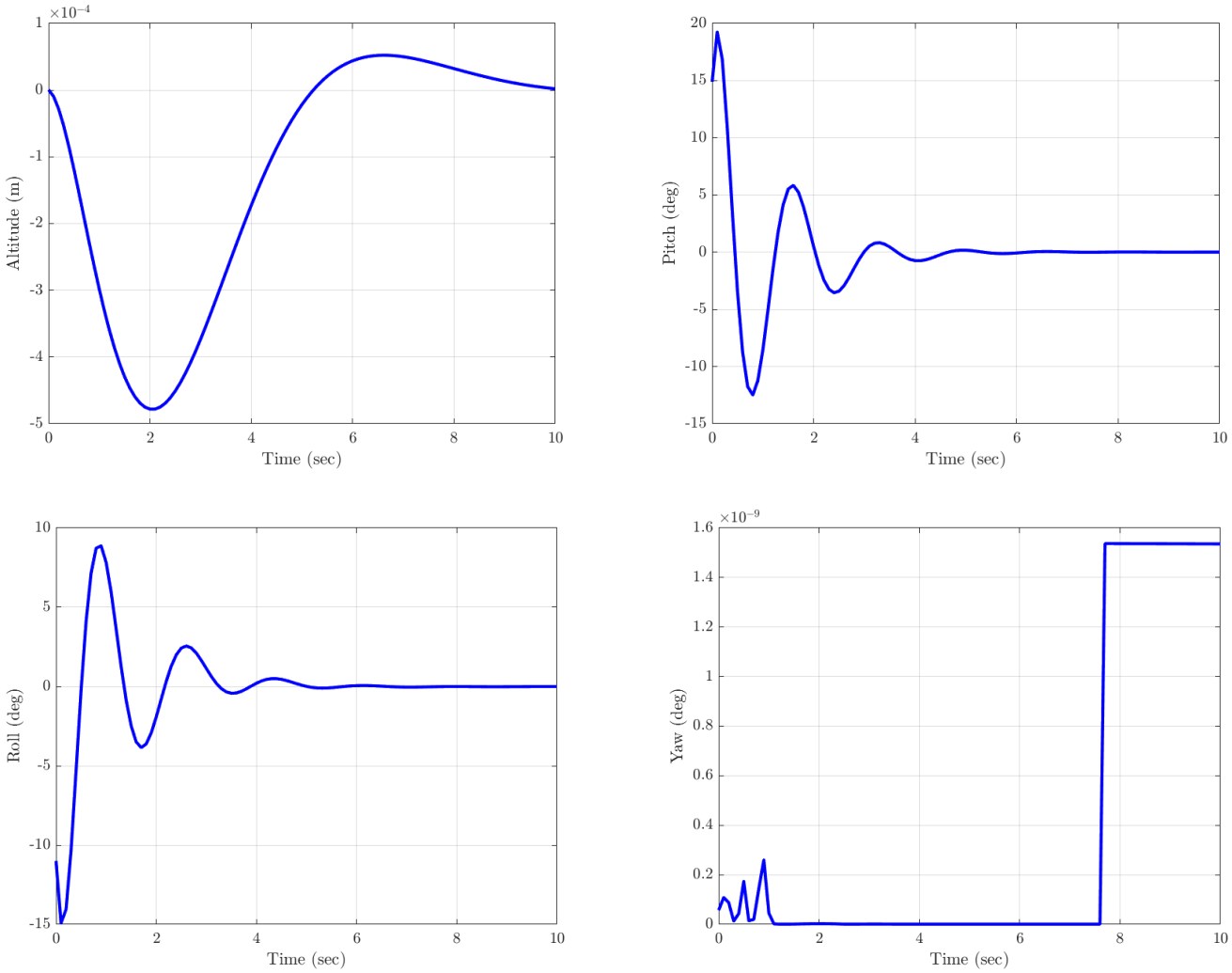

Fig. 5. Case 1: Input Demand to Access the Baseline Performance

real-world conditions, further substantiating the results obtained from nonlinear simulations.

Appendix A : State Space Matrices of Test Vehicle

The state space matrices and observer gain matrices for the MPC design are given below:

$$\bar{A} = \begin{bmatrix}
0 & 0 & 0 & 1 & 0 & 0 & 0 & 0 & 0 & 0 & 0 & 0 \\
0 & 0 & 0 & 0 & 1 & 0 & 0 & 0 & 0 & 0 & 0 & 0 \\
0 & 0 & 0 & 0 & 0 & 1 & 0 & 0 & 0 & 0 & 0 & 0 \\
0 & 0 & 0 & -0.1785 & 0 & 0 & 0 & -9.81 & 0 & 0 & 0 & 0 \\
0 & 0 & 0 & 0 & -0.1785 & 0 & 9.8100 & 0 & 0 & 0 & 0 & 0 \\
0 & 0 & -0.8169 & 0 & 0 & -1.2495 & 0 & 0 & 0 & 0 & 0 & 0 \\
0 & 0 & 0 & 0 & 0 & 0 & 0 & 0 & 0 & 1 & 0 & 0 \\
0 & 0 & 0 & 0 & 0 & 0 & 0 & 0 & 0 & 0 & 1 & 0 \\
0 & 0 & 0 & 0 & 0 & 0 & 0 & 0 & 0 & 0 & 0 & 1 \\
0 & 0 & 0 & 0 & 0 & 0 & -3.6594 & 0 & 0 & -1.7815 & 0 & 0 \\
0 & 0 & 0 & 0 & 0 & 0 & 0 & -3.6376 & 0 & 0 & -1.7709 & 0 \\
0 & 0 & 0 & 0 & 0 & 0 & 0 & 0 & -0.0785 & 0 & 0 & -0.2868
\end{bmatrix}$$

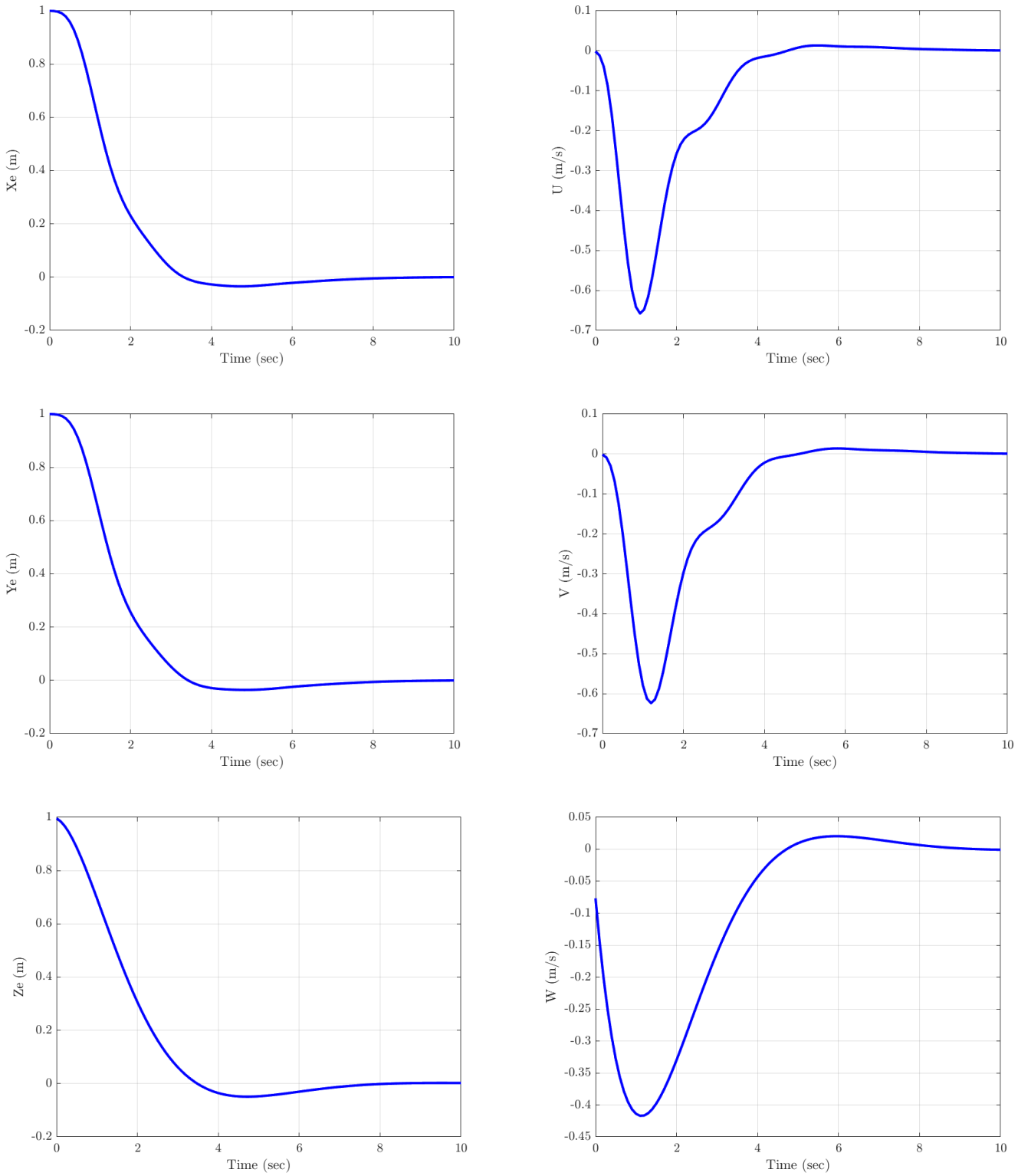

Fig. 6. Case 1: Outputs Performance

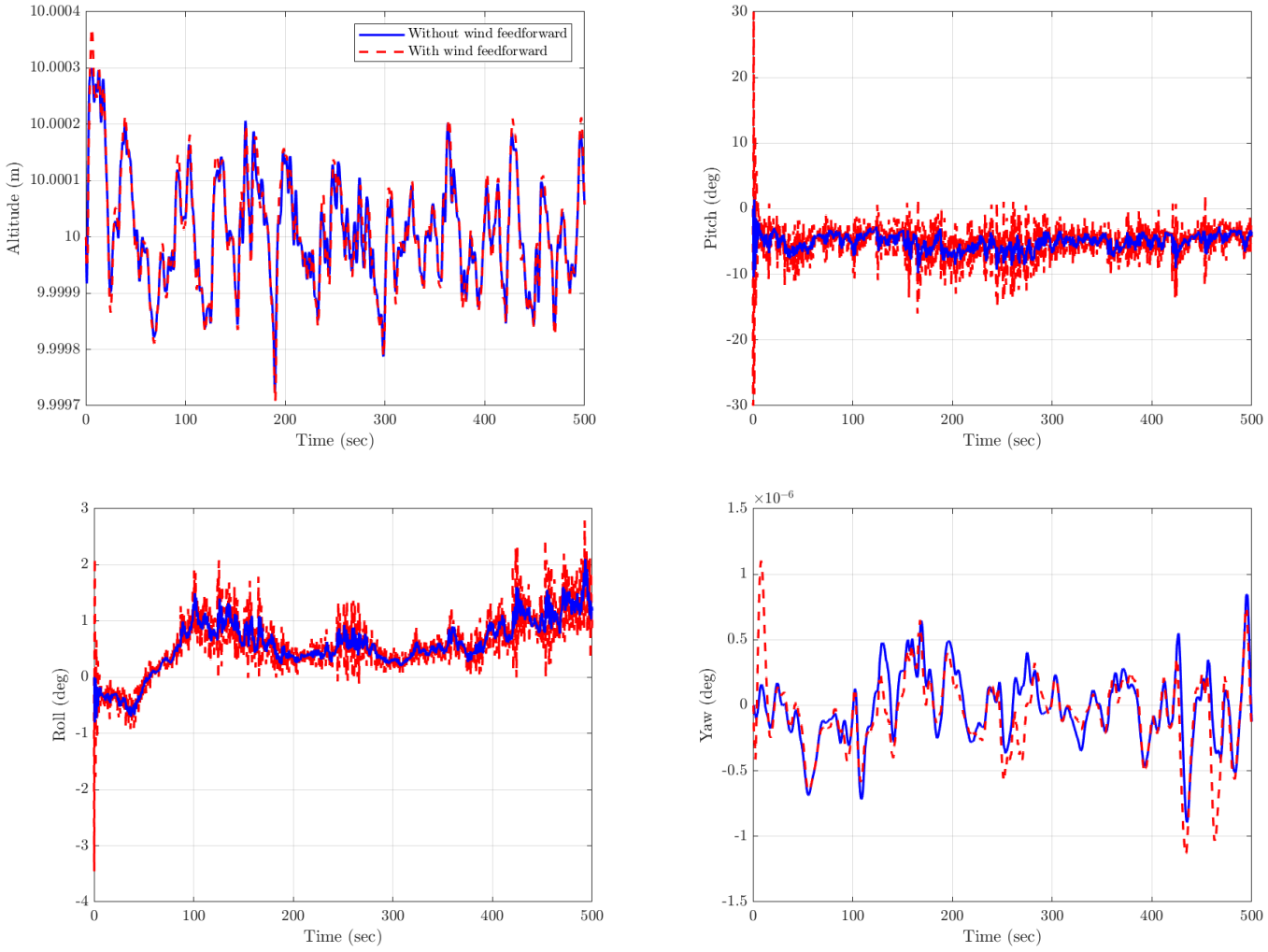

Fig. 7. Case 2: Input Demand to Compensate Wind Effects

$$\bar{B}_u = \begin{bmatrix} 0 & 0 & 0 & 0 & 0 & -0.8160 & 0 & 0 & 0 & 0 & 0 & 0 \\ 0 & 0 & 0 & 0 & 0 & 0 & 0 & 0 & 0 & 0 & 3.6376 & 0 \\ 0 & 0 & 0 & 0 & 0 & 0 & 0 & 0 & 0 & 3.6594 & 0 & 0 \\ 0 & 0 & 0 & 0 & 0 & 0 & 0 & 0 & 0 & 0 & 0 & 0.0785 \end{bmatrix}^T$$

$$\bar{B}_w = \begin{bmatrix} 0 & 0 & 0 & -0.1785 & 0 & 0 & 0 & 0 & 0 & 0 & 0 & 0 \\ 0 & 0 & 0 & 0 & -0.1785 & 0 & 0 & 0 & 0 & 0 & 3.6376 & 0 \\ 0 & 0 & 0 & 0 & 0 & -1.2495 & 0 & 0 & 0 & 3.6594 & 0 & 0 \end{bmatrix}^T$$

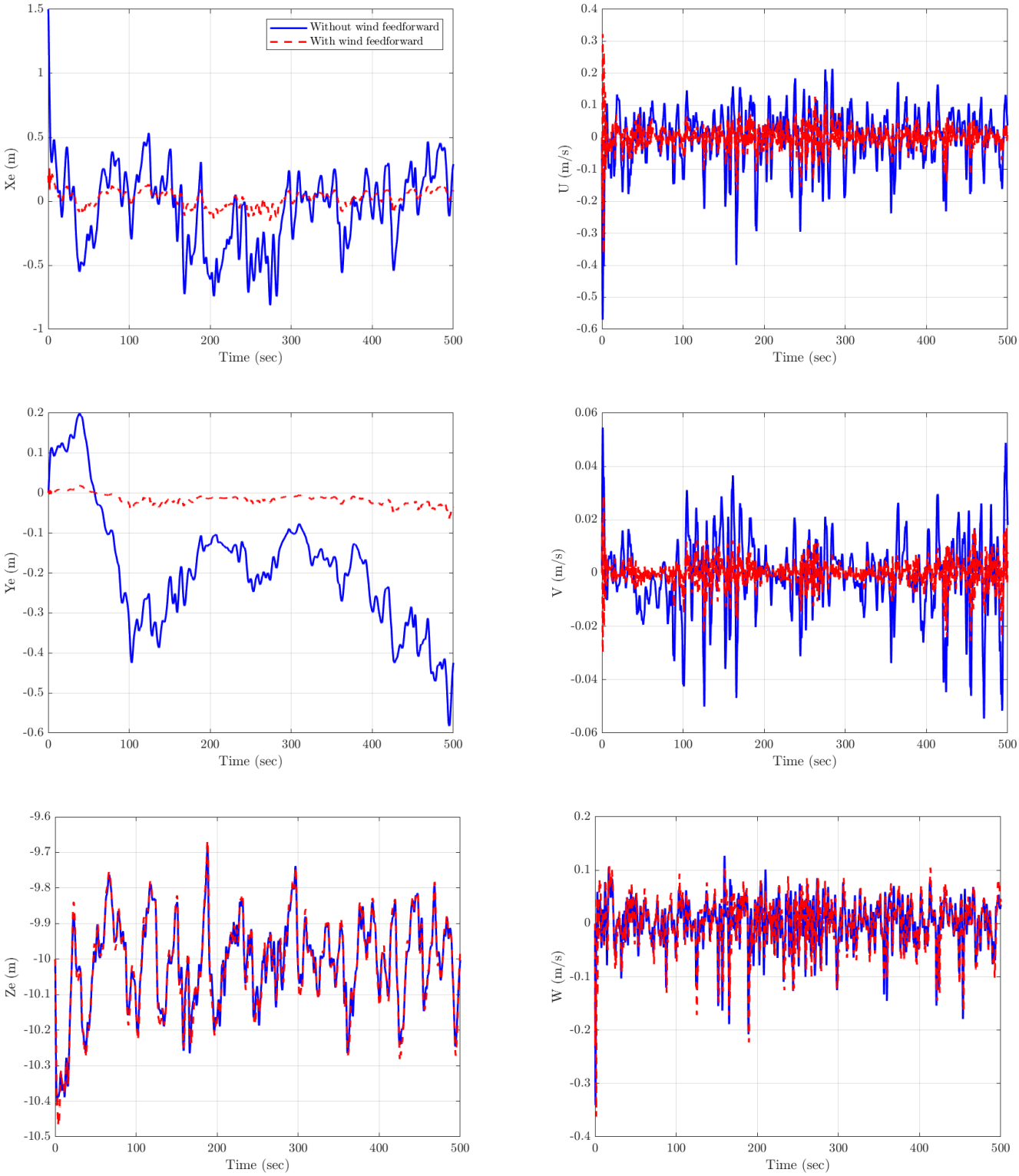

Fig. 8. Case 2: Wind Disturbance Compensated Output

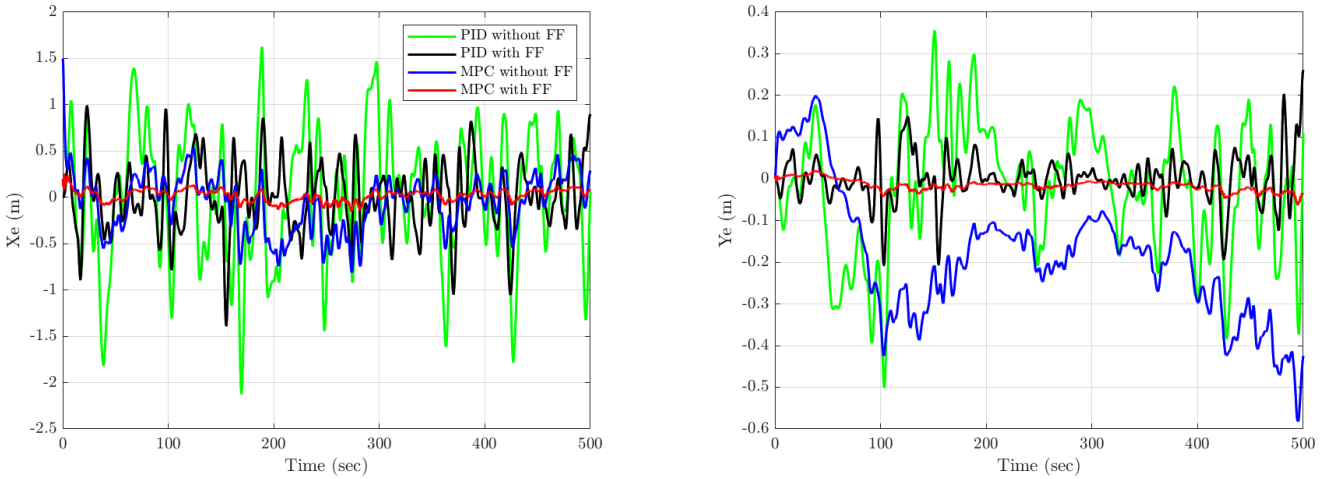

Fig. 9. Comparison of MPC with PID Control Law

$$L = \begin{bmatrix} 0.0822 & 0 & 0 & 0.0466 & 0 & 0 & 0 & -0.0009 & 0 \\ 0 & 0.0822 & 0 & 0 & 0.0466 & 0 & 0.0009 & 0 & 0 \\ 0 & 0 & 0.0003 & 0 & 0 & 0 & 0 & 0 & 0 \\ 0.0398 & 0 & 0 & 0.0659 & 0 & 0 & 0 & -0.0051 & 0 \\ 0 & 0.0398 & 0 & 0 & 0.0659 & 0 & 0.0051 & 0 & 0 \\ 0 & 0 & 0 & 0 & 0 & 0.0002 & 0 & 0 & 0 \\ 0 & 0.0003 & 0 & 0 & 0.0037 & 0 & 0.0009 & 0 & 0 \\ -0.0003 & 0 & 0 & -0.0037 & 0 & 0 & 0 & 0.0009 & 0 \\ 0 & 0 & 0 & 0 & 0 & 0 & 0 & 0 & 0.0001 \\ 0 & -0.0016 & 0 & 0 & -0.0057 & 0 & -0.0002 & 0 & 0 \\ 0.0016 & 0 & 0 & 0.0057 & 0 & 0 & 0 & -0.0002 & 0 \\ 0 & 0 & 0 & 0 & 0 & 0 & 0 & 0 & 0 \end{bmatrix}$$

References

[1] J. González-Rocha, C. A. Woolsey, C. Sultan and S. F. De Wekker, Sensing wind from quadrotor motion, *Journal of Guidance, Control, and Dynamics* **42**(4) (2019) 836–852.

[2] S. Waslander and C. Wang, Wind disturbance estimation and rejection for quadrotor position control, *AIAA Infotech@ Aerospace Conference*, (2009), p. 1983.

[3] Z. Xing, Y. Zhang, C.-Y. Su, Y. Qu and Z. Yu, Kalman filter-based wind estimation for forest fire monitoring with a quadrotor UAV, *2019 IEEE Conference on Control Technology and Applications (CCTA)*, IEEE (2019), pp. 783–788.

[4] J. Gonzalez-Rocha, C. A. Woolsey, C. Sultan, S. de Wekker and N. Rose, Measuring atmospheric winds from quadrotor motion, *AIAA Atmospheric Flight Mechanics Conference*, (2017), p. 1189.

[5] V. Ayala-Alfaro, F. Torres-Del Carmen and J.-P. Ramirez-Paredes, Wind field estimation by small UAVs for rapid response to contaminant leaks, *2020 International Conference on Unmanned Aircraft Systems (ICUAS)*, IEEE (2020), pp. 1546–1552.

[6] D. Shi, Z. Wu and W. Chou, Generalized extended state observer based high precision attitude control of quadrotor vehicles subject to wind disturbance, *IEEE Access* **6** (2018) 32349–32359.

[7] A. Aboudonia, A. El-Badawy and R. Rashad, Active anti-disturbance control of a quadrotor unmanned aerial vehicle using the command-filtering backstepping approach, *Nonlinear Dynamics* **90**(1) (2017) 581–597.

[8] S. I. Azid, K. Kumar, M. Cirrincione and A. Fagiolini, Wind gust estimation for precise quasi-hovering control of quadrotor aircraft, *Control Engineering Prac-*

tice **116** (2021) p. 104930.
[9] H. Yang, L. Cheng, Y. Xia and Y. Yuan, Active disturbance rejection attitude control for a dual closed-loop quadrotor under gust wind, *IEEE Transactions on Control Systems Technology* **26**(4) (2017) 1400–1405.
[10] J. Han, From PID to active disturbance rejection control, *IEEE Transactions on Industrial Electronics* **56**(3) (2009) 900–906.
[11] L. Thobois, J. P. Cariou and I. Gultepe, Review of lidar-based applications for aviation weather, *Pure and Applied Geophysics* **176**(5) (2019) 1959–1976.
[12] N. Fezans, J. Schwithal and D. Fischenberg, In-flight remote sensing and identification of gusts, turbulence, and wake vortices using a doppler lidar, *CEAS Aeronautical Journal* **8** (2017) 313–333.
[13] N. Vasiljević, M. Harris, A. Tegtmeier Pedersen, G. Rolighed Thorsen, M. Pitter, J. Harris, K. Bajpai and M. Courtney, Wind sensing with drone-mounted wind lidars: proof of concept, *Atmospheric Measurement Techniques* **13**(2) (2020) 521–536.
[14] P. Qi, X. Zhao and R. Palacios, Autonomous landing control of highly flexible aircraft based on lidar preview in the presence of wind turbulence, *IEEE Transactions on Aerospace and Electronic Systems* **55**(5) (2019) 2543–2555.
[15] M. Pichault, C. Vincent, G. Skidmore and J. Monty, Lidar-based detection of wind gusts: An experimental study of gust propagation speed and impact on wind power ramps, *Journal of Wind Engineering and Industrial Aerodynamics* **220** (2022) p. 104864.
[16] A. P. Mendez, J. F. Whidborne and L. Chen, Wind preview-based model predictive control of multi-rotor UAVs using lidar, *Sensors* **23**(7) (2023) p. 3711.
[17] M. Cook, *Flight Dynamics Principles — A Linear Systems Approach to Aircraft Stability and Control*, 3rd edn. (Butterworth-Heinemann, Oxford, U.K., 2013).
[18] V. M. Martinez, Modelling of the flight dynamics of a quadrotor helicopter, PhD thesis, Cranfield University, School of Engineering, Department of Aerospace Sciences (2007).
[19] A. P. Mendez, J. F. Whidborne and L. Chen, Experimental verification of an lidar based gust rejection system for a quadrotor UAV, *2022 International Conference on Unmanned Aircraft Systems (ICUAS)*, IEEE (2022), pp. 1455–1464.

Zohaib Latif received his B.S. degree in Electronic Engineering from Mohammad Ali Jinnah University, Islamabad, Pakistan, in 2014. He then pursued his M.S. and Ph.D. degrees in Electrical Engineering at the Capital University of Science and Technology, Islamabad, completing them in 2018 and 2023, respectively. During his Ph.D. studies, he was a visiting research student at the Centre for Aeronautics, Cranfield University, UK. His research interests include modeling and simulation, robust control, model predictive control, artificial intelligence, and their applications in aerospace systems.

James Whidborne (Senior Member, IEEE) received his BA in engineering from the Cambridge University, and MSc and PhD in systems and control from the University of Manchester Institute of Science and Technology (UMIST). From 1991 to 1994, he held a position of Research Associate with the Department of Engineering, University of Leicester. From 1994 to 2003, he was a Lecturer, then Senior Lecturer with the Department of Mechanical Engineering, Kings College London. He is currently the Head of the Dynamics Simulation and Control Group in the Centre for Aeronautics at Cranfield University. He has about 240 refereed research publications, including three books. He is a Chartered Engineer, a Member of the IET and a Senior Member of the IEEE. His research interests are in the theory and application of advanced control, particularly applied to flight control problems.

Aamer Iqbal Bhatti (Senior Member, IEEE) received the M.S. degree in control systems from Imperial College London, London, U.K., in 1994, and the Ph.D. degree in control engineering from Leicester University, Leicester, U.K., in 1998. From 2007 to 2023, he was a Professor with the Department of Electrical Engineering, Capital University of Science and Technology, Islamabad, Pakistan. He is currently a Professor with the Control and Instrumentation Engineering Department, King Fahd University of Petroleum & Minerals, Dhahran, Saudi Arabia. His research areas include GSR development, radar signal processing, line Echo canceller design, GSM audio codes, dynamic system modeling, and large diesel systems.

Amir Shahzad received the M.S. degree in Astrodynamics from University of Surrey, Guildford, U.K in 2004 and PhD degree in control systems engineering from Imperial College London in 2010. He is currently working in Centre of Excellence in Science and Applied Technologies, Islamabad. His research interests include modelling and simulation, robust control, model predictive control, optimisation and their applications in aerospace systems.

Raza Samar (Member, IEEE) received the B.Sc. degree in electrical engineering from the University of Engineering and Technology Lahore, Lahore, Pakistan, in 1990, the M.S. degree in electrical engineering from Stanford University, Stanford, CA, USA, in 1992, and the Ph.D. degree in control systems engineering from the University of Leicester, Leicester, U.K., in 1995. He is currently working in Centre of Excellence in Science and Applied Technologies, Islamabad. His research interests include optimal and robust control applications, linear estimation, intelligent control, and application of optimization to industrial and aerospace problems. Dr. Raza is a lifetime and a senior member of the American Institute of Aeronautics and Astronautics (AIAA).

Enhancing quadrotor resilience in outdoor operations with real-time wind gust measurement by using LiDAR

Latif, Zohaib

2025-03-12

Latif Z, Whidborne JF, Bhatti AI, et al., (2025) Enhancing quadrotor resilience in outdoor operations with real-time wind gust measurement by using LiDAR. Unmanned Systems, Available online 12 March 2025

https://doi.org/10.1142/s2301385026500081